Available online at www.sciencedirect.com
ScienceDirect
International Journal of Heat and Mass Transfer 51 (2008) 41–51
International Journal of HEAT and MASS TRANSFER
www.elsevier.com/locate/ijhmt

Analysis of the mass transfer controlled regime in automotive catalytic converters

H. Santos [a], M. Costa [b,*]

[a] Mechanical Engineering Department, School of Technology and Management, Polytechnic Institute of Leiria, Leiria, Portugal
[b] Mechanical Engineering Department, Instituto Superior Técnico, Technical University of Lisbon, Lisboa, Portugal

Received 29 December 2006
Available online 16 July 2007

Abstract

This article concentrates on the analysis of the mass transfer controlled regime in automotive catalytic converters operating under real conditions. The main objective of the work reported is to evaluate the performance of the existing correlations for the mass transfer rate, expressed as the Sherwood (*Sh*) number, against new experimental data and, if necessary, to establish new correlations that can be used in 1D two-phase models. The experiments have included measurements of conversion efficiencies for hydrocarbons, CO and NO_x from ceramic and metallic three way catalytic converters. The present data show that the calculated *Sh* are always below the asymptotic *Sh*. This indicates that, in addition to the external mass transfer limitation, both kinetics and internal pore diffusion limitations in the washcoat also contribute to reduce the catalytic converter performance even at high temperatures. In addition, the experimental data reveals that *Sh*'s are chemical species dependent, which, to the best of our knowledge, has not been reported previously. The following correlations for the mass transfer rate were obtained from the experiments: $Sh_{HC} = 0.6272(ReSc_{HC}\frac{d}{L})^{0.934}$, $Sh_{CO} = 0.9260(ReSc_{CO}\frac{d}{L})^{1.078}$ and $Sh_{NO_x} = 1.2824(ReSc_{NO_x}\frac{d}{L})^{1.079}$.
© 2007 Elsevier Ltd. All rights reserved.

Keywords: Three-way catalytic converter; Mass transfer; Sherwood number; Experimental correlation

1. Introduction

The introduction of emissions legislation in the early 1970s has accelerated research into all areas of automotive exhaust gas catalysis. Currently, the two most common catalysts available in the market are ceramic and metallic substrates [1]. In both cases, the substrate wall is treated with a 10–150 μm thick porous layer (washcoat) containing catalysts supports, stabilizers and promoters, where the active metal sites are dispersed by impregnation. Within this washcoat, the reactants diffuse and react on the active catalyst sites.

A number of models have been proposed to describe the coupling between the mass, heat and chemical reaction in automotive catalytic converters. Classical one-dimensional (1D) models of automotive catalysts with simplified representation of the fluid flow through the device have proven their effectiveness in designing catalyst systems [2]. A major simplification of these models is to represent the whole matrix by a single channel with the assumption of equivalent passages with no interaction. These models assume that the catalyst is perfectly insulated and that it is exposed to a uniform flow. The effects of thermal gradients in the radial direction are presumed to be insignificant and the temperature and concentration profiles are assumed to be the same in all channels. This allows the entire catalysts to be modeled with only one channel.

The model formulation depends on the system or device where modeling is applied as well as the design parameters under investigation. The full reactor model requires a strong computational time which would make it nearly impossible for full transient regulatory cycle [2]. In addition,

* Corresponding author. Tel.: +351 218417378; fax: +351 218475545.
E-mail address: mcosta@ist.utl.pt (M. Costa).

0017-9310/$ - see front matter © 2007 Elsevier Ltd. All rights reserved.
doi:10.1016/j.ijheatmasstransfer.2007.04.044

Nomenclature

A_Ω	cross-sectional area of the channel [m^2]
$\frac{A}{V}$	mass transfer area per unit of the catalyst volume [m^{-1}]
C	surface roughness constant
C_i	concentration of the chemical specie i [mol m^{-3}]
$C_{0,i}$	concentration of the chemical specie i at the channel inlet [mol m^{-3}]
$C_{w,i}$	concentration of the chemical specie i at the surface of the washcoat [mol m^{-3}]
d	hydraulic diameter of the monolith cell channel [m]
$D_{m,i}$	molecular diffusion of the reacting specie i [m^2 s^{-1}]
L	length of the channel [m]
$k_{m,i}$	mass transfer coefficient from the bulk gas to the washcoat surface [m s^{-1}]
$k_{S,i}$	effective surface rate constant of the reacting specie i [m s^{-1}]
$k_{V,i}$	reaction rate constant per volume of the washcoat [s^{-1}]
NTU, NTU_i	number of transfer units
P_i	transverse Peclet number
Pe_i	axial Peclet number
P_Ω	wetted perimeter of the channel [m]
R_Ω	effective transverse diffusion length [m], ($R_\Omega = A_\Omega/P_\Omega$)
R^2	correlation coefficient
Re	Reynolds number
Sc_i	Schmidt number
Sh, Sh_i	Sherwood number
$Sh_{T\infty}$	asymptotic Sherwood number at constant wall temperature
t_c	convection (residence) time [s]
$t_{d,i}$	transverse diffusion time [s]
$t_{z,i}$	longitudinal diffusion time [s]
$t_{R,i}$	wall reaction time [s]
v	flow velocity in the longitudinal direction [m s^{-1}]
w	volumetric washcoat loading per volume catalyst
z	axial length [m]

Greek symbols

δ_C	effective washcoat thickness [m]
$\phi^2_{S,i}$	square of transverse Thiele modulus
η	effectiveness factor of the reaction in the washcoat
ν_g	kinematic viscosity of the exhaust gas mixture [m^2 s^{-1}]

Subscript

i	chemical specie i

full reactor model requires velocity and temperature profiles at the inlet of the catalytic converter. Such data are usually unavailable in routine engine-bench or driving cycle converter tests, which are the main application field of automotive catalytic converters models. In these cases, accuracy may be slightly sacrificed because of constraints such as simplicity or flexibility. Under these circumstances, the single channel modeling approach is preferable for these application-oriented models [3].

The mass or heat transfer within a single channel can be described by two inherently coupled processes: external transfer from the bulk to the substrate and internal transfer inside the porous washcoat as illustrated in Fig. 1. Hence, the behavior of a single channel can be mathematically described by a convection–diffusion equation in the fluid phase coupled with the diffusion-reaction equation within the washcoat involving more than one spatial dimension. Instead, the monoliths have been studied by decoupling the above two process while lumping the effect of washcoat diffusion into the known effectiveness factor. This has resulted in two broadly classified hierarchical models: two-dimensional (2D) convection–diffusion models with wall reaction [4] and 1D two-phase models [2,3,5]. Over the years, 1D two-phase models, which are derived by averaging the full model over the channel cross section, became more popular not only because of their simplicity but also because of the less computational time required for the solution.

External mass transfer is especially important when modeling catalytic converters. The 1D models require the averaging of the radial concentration and temperature of the fluid. This creates a discontinuity at the wall that is

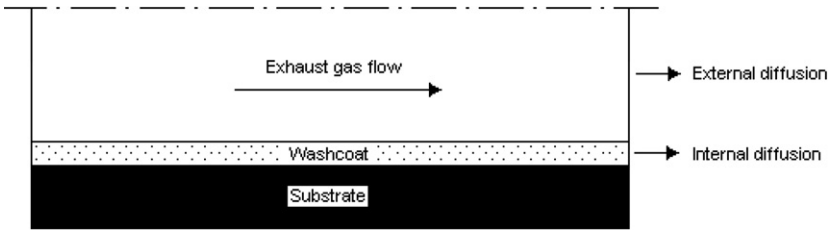

Fig. 1. Schematic representation of a single channel.

accounted for by introducing heat and mass transfer coefficients into the model. The transfer coefficients that appear in the 1D two-phase models depend on various system parameters, such as shape and dimensions of the channel, kinetic parameters, fluid and washcoat proprieties and are often expressed in terms of dimensionless numbers, specifically the Sherwood (Sh) and the Nusselt (Nu) numbers. In the 2D case, it is possible to impose correctly the flux boundary condition, and thus the need for heat and mass transfer correlations does not exist.

The literature reveals a number of different correlations concerning the mass transfer coefficient in monolithic reactors [6–10]. In fact, the existing correlations for the mass transfer coefficients differ significantly and there is no established consensus as to which, if any, is correct. Since Sherwood numbers can have a significant effect on the predicted emissions for automotive catalysts, accurate knowledge of mass transfer coefficients is thus essential for 1D mathematical modeling of their performance. Against this background, the choice of proper correlations for the evaluation of heat and mass transfer coefficients is a critical point for the adequacy of 1D model predictions [11].

Hawthorn [6] recognized the need to determine heat and mass transfer coefficients in order to model the performance of afterburner catalysts. Using the analytical solutions presented by Kays and London [12] for fully developed flow and based on the numerical analysis of laminar flow in ducts, Hawthorn [6] proposed the following semi-analytical equation for the average Sherwood number (Sh) in a monolith channel with laminar flow and developing boundary layers:

$$Sh = Sh_{T\infty}\left(1 + CReSc\frac{d}{L}\right)^{0.45} \quad (1)$$

where $Sh_{T\infty}$ is a constant that depends on the geometry of the transverse section of the monolith channel, and corresponds to an asymptotic Sherwood number for zero concentration at the wall, that is, constant temperature at the wall. For automobile monolith catalysts, the value of the constant C is taken equal to 0.095.

Several experimental correlations for the external mass transfer coefficient of monolith catalysts have been reported in the literature. Table 1 identifies the main contributions, including a summary of the test conditions used in each study. Votruba et al. [7] measured the rates of evaporation of water and a number of hydrocarbons from the surface of porous monolith structures. These authors verified that Eq. (1) did not provide a good fit of their data and developed the following empirical correlation:

$$Sh = 0.705\left(Re\frac{d}{L}\right)^{0.43} Sc^{0.56} \quad (2)$$

Votruba et al. [7] concluded that although this correlation could be used for the design of after-burner reactors, there was still a need for further experimental data.

Bennett et al. [8] reported mass transfer coefficients for the oxidation of propane (C_3H_8) within a monolith catalyst along with the following correlation:

$$Sh = 0.0767\left(1 + ReSc\frac{d}{L}\right)^{0.829} \quad (3)$$

These authors verified that Eq. (1) overestimated their mass transfer rates by a factor of 20, whereas Eq. (2) overestimated their measured values by a factor of 3.

Ullah et al. [9] conducted experiments with ceramic and metallic substrates to measure mass transfer coefficients under reacting conditions (CO oxidation) and obtained the following correlation:

$$Sh = 0.766\left(ReSc\frac{d}{L}\right)^{0.483} \quad (4)$$

The values reported by Ullah et al. [9] for Sherwood agreed well with those predicted by Eq. (2).

Hatton et al. [10] reported hydrocarbons (HC) and CO concentration data measured at the inlet and outlet of ceramic square monolith channels with rounded corners, and the calculated Sh's were used to obtain the following equation:

$$Sh = 0.6024\left(ReSc\frac{d}{L}\right)^{0.716} \quad (5)$$

These investigators verified that the overall conversion efficiency of the after-treatment system was not solely mass transfer controlled and they suggested that chemical kinetics play a role in the Sherwood number relationship found.

Shamim [13] investigated the influence of the heat and mass transfer coefficients on the performance of automotive catalytic converters, and concluded that catalyst performance is influenced by both heat and mass transfer phenomena, with mass transfer playing a more substantial role. This investigator showed that cumulative CO emission decreases by about 73% when Sh is increased from 1 to 10. Hatton et al. [10] also showed that the use of different Sherwood numbers could lead up to 55% difference in the predicted cumulative emissions of HC, CO and NO_x. This result clearly emphasizes the importance of the accurate modeling of the mass transfer phenomenon.

In spite of the large use of the correlation of Votruba et al. [7] in 1D modeling studies for automotive applications, *e.g.* [3,14,15], the validity of Eq. (2) under reacting conditions has not yet been thoroughly established. Other modeling studies such as those of Guojiang and Song [16] and Koltsakis et al. [5] have adopted the correlations of Ullah et al. [9] and Hawthorn [6], respectively. All these modeling studies demonstrate that there are not consensuses on the correlation to be used.

In this context, the main goal of the present study was to evaluate the performance of the existing correlations against new experimental data and, if necessary, to establish new correlations for Sh that can be used in 1D

Table 1
Summary of the test conditions and correlations derived for the Sherwood number for various studies

Reference	d (mm)	L (mm)	Re	Sc	$ReSc(d/L)$	Temperature (K)	Probe reaction	Feed stream	Catalytic converter	Correlation
Votruba et al. [7]	1–10	12–40	3–480	0.6–3.28	1.2–1312	(not available)	(not applied)	H_2O and HC evaporation	(not applied)	$Sh = 0.705\left(Re\frac{d}{L}\right)^{0.43} Sc^{0.56}$
Bennett et al. [8]	1	3, 6, 20, 38	13.5–45	1.21	1.21–18.15	680–800	C_3H_8 oxidation	1000 ppm C_3H_8 in air	Ceramic 62 cells/cm^2	$Sh = 0.0767\left(1 + ReSc\frac{d}{L}\right)^{0.829}$
Ullah et al. [9]	1	20, 30, 40, 50, 150	–	0.98	0.8–130	473–673	CO oxidation	0.5% CO and 0.25% O_2 in N_2	Metallic and ceramic 31, 47, 62 cells/cm^2	$Sh = 0.766\left(ReSc\frac{d}{L}\right)^{0.483}$
Hatton et al. [10]	1	100	–	–	0.5–3.70	583–873	CO and HC oxidation	Four stroke spark ignition exhaust gases mixture	Ceramic three way converter 62 cells/cm^2	$Sh = 0.6024\left(ReSc\frac{d}{L}\right)^{0.716}$
Present work	0.969	120	33.3–148.2	–	0.17–1.38	638–1074	CO and HC oxidation and NO_x reduction	Four stroke spark ignition exhaust gases mixture, see [15]	Metallic three way converter 62 cells/cm^2	$Sh_{HC} = 0.6272\left(ReSc_{HC}\frac{d}{L}\right)^{0.934}$ $Sh_{CO} = 0.9260\left(ReSc_{CO}\frac{d}{L}\right)^{1.078}$
	1.105	120	44.9–199.5	–	0.26–2.11	638–1074	CO and HC oxidation and NO_x reduction	Four stroke spark ignition exhaust gases mixture, see [15]	Ceramic three way converter 62 cells/cm^2	$Sh_{NO_x} = 1.2824\left(ReSc_{NO_x}\frac{d}{L}\right)^{1.079}$

two-phase models and, thereby, improve the reliability of these models. The experiments have included measurements of conversion efficiencies for HC, CO and NO_x from ceramic and metallic three way catalytic converters operating under real automotive conditions.

2. Instrumentation and test procedures

This section describes the experiments performed in order to measure the mass transfer coefficients in monoliths under reacting conditions. All experiments were carried out with temperatures above the light-off temperature where the performance of the units is controlled mainly by external mass transfer of the exhaust gas to the catalyst surface. The present experimental procedure was similar to that used by Bennett et al. [8], Ullah et al. [9] and Hatton et al. [10].

The measurements reported here were carried out on a vehicle equipped with a 2.8 L DOHC V6 spark ignition engine that has multipoint fuel injection. Table 2 lists the main characteristics of the engine. The vehicle was tested on a chassis dynamometer (Maha LPS200) under steady-state conditions for a variety of operating conditions in order to measure the catalytic converters conversion efficiencies. In this study, two commercial catalysts have been used and Table 3 lists their main characteristics. In order to perform the experiments, each catalyst was in turn placed in the so called under-floor position replacing the original three way catalytic converter installed on the vehicle.

Engine control on-line data was monitored using a Bosch KTS 500 engine diagnostic scanner connected to a diagnostic link, located within the vehicle below the dashboard. The scanner provided the following engine parameters: intake mass air flow (g/s), intake air temperature (°C), coolant temperature (°C), engine speed (rpm), throttle position (%) and spark advance (°), among others.

Fig. 2 shows a schematic of the vehicle exhaust system and associated instrumentation for the measurements of the gas emission data upstream and downstream of the catalytic converter. Exhaust gas was sampled from the exhaust pipe through stainless steel probes with the aid of the suction pump as shown in Fig. 2. The analytical instrumentation included a magnetic pressure analyzer for O_2 measurements, non dispersive infrared gas analyzers for CO_2 and CO measurements, a flame ionization detector for HC measurements and a chemiluminescent analyzer for NO_x measurements. Zero and span calibrations with standard mixtures were performed before and after each measurement session. The maximum drift in the calibration was within ±2% of the full scale.

Fig. 3 shows a schematic of the type K thermocouples location in the vehicle exhaust system for the measurement of the temperatures of the exhaust gases and of the substrate wall. As can be seen in the figure, thermocouples T1 and T6 allowed for the measurement of the exhaust gas temperature upstream and downstream of the catalytic converter, and thermocouples T2, T3, T4 and T5 allowed for the measurement of the substrate wall temperatures. Finally, thermocouple T7 allowed for the measurement of the temperature of the gases at exit of exhaust manifold.

Table 4 summarizes the test conditions for which the present study was carried out. The engine was tested under steady-state operating conditions (*i.e.*, after engine warm-up). For each engine speed (2000, 3000 and 4000 rpm) tests were made for six different loads (BMEP – break

Table 2
Main engine characteristics

Number of cylinders	6
Displacement (cm^3)	2792
Bore (mm)	81
Stroke (mm)	90.3
Compression ratio	1:10
Injection system	Motronic M 3.8.1
Number of valves	12 (2 per cylinder)

Table 3
Main technical attributes of the catalysts studied

(a) Geometrical properties		
Substrate type	Sinusoidal cell metallic	Square cell ceramic
Cell density (cells/cm^2)	62 (400 cpsi)	
Substrate dimensions (mm)	Diameter = 127; L = 120	
Catalyst volume (dm^3)	1.52	
Uncoated geometric surface area (m^2/m^3)	3684	2740
Coated geometric surface area (m^2/m^3)	3220	2526
Uncoated wall thickness (mm)	0.0508 (2 mil)	0.1651 (6.5 mil)
Mean washcoat thickness (mm)	0.019	0.025
Open frontal area uncoated (%)	89.3	75.7
Open frontal area coated (%)	82.6	69.0
Cell hydraulic diameter uncoated (mm)	0.9694	1.105
(b) Physical properties of substrates		
Specific heat capacity of substrate (J/kgK)	463	719
Density of substrate (kg/m^3)	7650	1770
Bulk density of substrate (kg/m^3)	820	430
Substrate mass (g)	1165	628
Heat capacity of substrate (J/Kdm^3)	390	326
Thermal conductibility (W/mK)	13	1
(c) Physical properties of washcoat		
Washcoat material	CeO_2–Al_2O_3	
Specific heat capacity of washcoat (J/kgK)	950	
Density of washcoat (kg/m^3)	2790	
Bulk density of washcoat (kg/m^3)	185	
Washcoat mass (g)	281.2	
Heat capacity of washcoat (J/Kdm^3)	175.75	
Thermal conductibility of washcoat (W/mK)	1	
(d) Precious metals		
Precious metal loading	7 Pd/1 Rh	
Total mass of precious metal (g)	1.159	

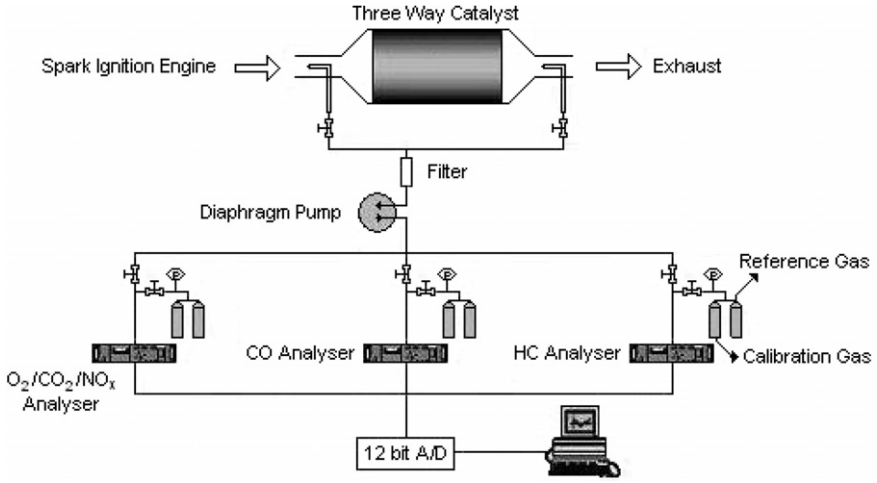

Fig. 2. Schematic of the vehicle exhaust system and associated instrumentation for the measurement of the gas emission data upstream and downstream of the catalytic converter.

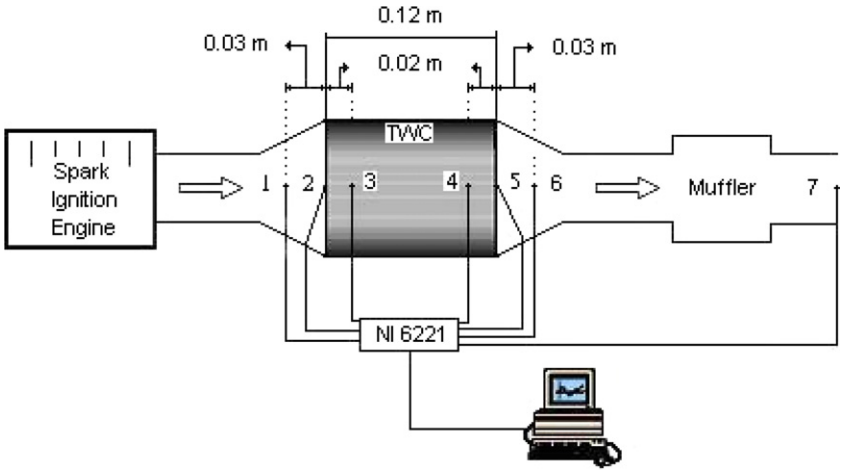

Fig. 3. Schematic of the thermocouples location in the vehicle exhaust system for the measurement of the temperatures of the exhaust gases and of the substrate wall.

Table 4
Test conditions

Engine speed (rpm)	BMEP (bar)	*Re*	P_{HC}	Pe_{HC}	P_{CO}	Pe_{CO}	P_{NOx}	Pe_{NOx}
Vehicle		*Metallic three way catalyst*						
2000	0.00–2.91	33.3–67.9	0.021–0.041	5901.2–9981.5	0.012–0.024	2940.6–5765.2	0.010–0.021	2568.5–5035.7
3000	0.00–4.49	48.7–115.4	0.030–0.067	7269.6–16530.3	0.017–0.039	4198.8–9547.6	0.015–0.034	3667.6–8339.6
4000	0.00–5.25	64.3–148.2	0.039–0.086	9442.2–21113.2	0.023–0.050	5453.7–12194.6	0.019–0.043	4763.6–10651.7
Vehicle		*Ceramic three way catalyst*						
2000	0.00–2.91	44.9–91.4	0.032–0.062	6005.3–11777.7	0.018–0.036	3496.5–6855.1	0.016–0.031	3029.7–5939.9
3000	0.00–4.49	65.6–155.3	0.045–0.103	8574.9–19498.3	0.026–0.060	4992.6–11352.7	0.023–0.052	4326.0–9837.0
4000	0.00–5.25	86.6–199.5	0.059–0.132	11137.5–24904.0	0.034–0.077	6484.7–14500.1	0.030–0.067	5618.9–12564.2

mean effective pressure). In order to establish steady-state operating conditions, the vehicle was operated continuously at a given speed and load for 20–30 min before each measurement session.

3. The one-dimensional model

The processes occurring in a catalytic converter are very complex, involving fluid mechanics, heat and mass transfer

and catalytic reactions. To characterize the flow and the reactions the following four characteristic times are used:

$$t_c = \frac{L}{v} \tag{6a}$$

$$t_{d,i} = \frac{(R_\Omega)^2}{D_{m,i}} \tag{6b}$$

$$t_{z,i} = \frac{L^2}{D_{m,i}} \tag{6c}$$

$$t_{R,i} = \frac{(R_\Omega/4)}{k_{S,i}} \tag{6d}$$

Note that the convection time is the same for the three chemical species under evaluation (HC, CO and NO_x); however, this is not true for both the transverse and the axial diffusion times as well as for the wall reaction time because the diffusion and the reaction times are dependent of the chemical species.

The above characteristic times lead to the following three independent dimensionless groups:

$$P_i = \frac{t_{d,i}}{t_c} = \frac{R_\Omega^2 v}{D_{m,i} L} \tag{7a}$$

$$Pe_i = \frac{t_{z,i}}{t_c} = \frac{vL}{D_{m,i}} \tag{7b}$$

$$\phi_{S,i}^2 = \frac{t_{d,i}}{t_{R,i}} = \frac{4R_\Omega k_{S,i}}{D_{m,i}} \tag{7c}$$

where the transverse Peclet number (P_i) represents the ratio of transverse diffusion time to convection time, the axial Peclet number (Pe_i) represents the ratio of axial diffusion time to convection time and the square of transverse Thiele modulus ($\phi_{S,i}^2$) – also referred as the local Damköhler number – represents the ratio of transverse diffusion time to the wall reaction time.

In addition, the definitions of three classical dimensionless groups used in this work are as follows:

$$Re = \frac{vd}{\nu_g} \tag{8a}$$

$$Sc_i = \frac{\nu_g}{D_{m,i}} \tag{8b}$$

$$Sh_i = \frac{k_{m,i} d}{D_{m,i}} \tag{8c}$$

According to Eqs. (7) and (8), the diffusion coefficients of the HC, CO and NO_x in the exhaust gas mixture have to be calculated. To carry out the calculations of the diffusion coefficients has been used the procedure described in McCullough et al. [17].

The dimensionless numbers Re, P_i and Pe_i are function of variables which are directly (the hydraulic diameter, d) or indirectly (the effective transverse diffusion length, R_Ω, and the flow velocity, v) dependent of the geometrical proprieties of the substrates, see Eqs. (7) and (8). Table 4 shows that the ceramic substrate has higher Re, P_i and Pe_i values as compared with the metallic substrate as a result of the different geometrical properties of the substrates. Specifically, Re, P_i and Pe_i are 34.6%, 53.2% and 18.9%, respectively, higher for the ceramic substrate as compared with the metallic substrate for each operating condition.

The flow regime in the exhaust manifold is turbulent [3]. Within the channels of the catalytic converter, however, the Reynolds number indicates that the flow is laminar [18] – for the present study Re is less than 200 for all tested conditions (see Table 4). It is well known that laminar flow is less favorable as compared with turbulent flow for external mass transfer. The transition of flow regime (*i.e.*, from turbulent in exhaust manifold to laminar within channels of the monolith) occurs few millimeters after the entrance in the monolith channels, that is, after the entrance region, the flow is fully developed in all extension of the monolith channels. The transport of the chemical gas species to the surface of the monolith is guaranteed mainly by diffusion ($P_i \leqslant 0.132$ for the present study), while the axial transport is primarily guaranteed by convection ($Pe_i \geqslant 2568.5$ for the present study).

The Sherwood number is calculated from the experimental data using a 1D two-phase model. For this model, the mass balance for the gas phase is expressed as:

$$v\frac{\partial C_i}{\partial z} = -k_{m,i}\frac{A}{V}(C_i - C_{w,i}) \tag{9}$$

For steady state operation, the rate of mass transfer to the surface of the washcoat must be equal to the rate of consumption by reaction within the washcoat. In this case, with a first order reaction, the mass balance for the solid phase is:

$$k_{m,i}\frac{A}{V}(C_i - C_{w,i}) = \eta w k_{V,i} C_{w,i} \tag{10}$$

Eq. (10) can be rewritten in the following form:

$$k_{m,i}(C_i - C_{w,i}) = \eta \delta_C k_{V,i} C_{w,i} \tag{11}$$

where δ_C is the effective washcoat thickness defined as the washcoat volume over the solid–fluid interfacial area.

Eq. (11) can be written as follows:

$$\frac{C_{w,i}}{C_i} = \frac{1}{1 + \frac{\eta \delta_C k_{V,i}}{k_{m,i}}} \tag{12}$$

Note that $k_{S,i}$ is related with $k_{V,i}$ through the following equation:

$$k_{S,i} = \eta \delta_C k_{V,i} \tag{13}$$

Using the definitions of $\phi_{S,i}^2$ Eq. (7c) and Sh_i Eq. (8c), results:

$$\frac{\eta \delta_C k_{V,i}}{k_{m,i}} = \frac{\phi_{S,i}^2}{Sh_i} \tag{14a}$$

or

$$\frac{k_{S,i}}{k_{m,i}} = \frac{\phi_{S,i}^2}{Sh_i} \tag{14b}$$

The relative magnitude of $\phi_{S,i}^2$ and Sh_i in Eq. (14) are indicative of the resistances offered by kinetics plus internal pore diffusion, and external mass transfer, respectively. The number of theoretical mass transfer units of a monolith catalyst can be found by assuming that the rate of catalytic reaction is infinite, *i.e.*, $C_{w,i} = 0$. In these conditions, the conversion efficiency is controlled solely by external mass transfer process. Under such conditions, the integration of Eq. (9) gives the following equation:

$$C_i = C_{0,i} \exp\left(-\frac{k_{m,i}\frac{A}{V}z}{v}\right) \tag{15}$$

From Eq. (15) the number of theoretical mass transfer units or number of transfer units (NTU) for the substrate can be defined as:

$$\mathrm{NTU}_i = \frac{k_{m,i}\frac{A}{V}z}{v} \tag{16}$$

Following the same reasoning, by knowing the conversion in a given catalyst, one can calculate the number of equivalent mass transfer units to evaluate the influence of the kinetics and internal pore diffusion limitations.

Rearranging Eq. (15) and using the Eq. (16), one can write:

$$\ln\left(\frac{C_i}{C_{0,i}}\right) = -\mathrm{NTU}_i \tag{17}$$

Using the definitions of the Reynolds, Schmidt and Sherwood numbers (Eqs. (8)), Eq. (17) can be rewritten as follows:

$$\ln\left(\frac{C_i}{C_{0,i}}\right) = -\frac{Sh_i\frac{A}{V}z}{ReSc_i}, \tag{18}$$

Rearranging Eq. (18), one gets for Sh_i:

$$Sh_i = -\frac{ReSc_i}{\frac{A}{V}z}\left[\ln\left(\frac{C_i}{C_{0,i}}\right)\right] \tag{19}$$

or, using Eq. (17), Eq. (19) becomes:

$$Sh_i = \frac{ReSc_i}{\frac{A}{V}z}\mathrm{NTU}_i \tag{20}$$

Eq. (20) permits to calculate the Sherwood number when the concentration at surface wall is exactly zero, that is, when the conversion efficiency is controlled only by external mass transfer process. Should this condition not be guaranteed, Eq. (20) will provide a Sherwood number lower than the asymptotic *Sh* [19].

4. Results and discussion

Modeling studies (e.g., [19]) shows that, after monolith ignition, the reaction is very fast so that the wall concentration of the reacting species is close to zero along the surface of the channel. Thus for this case the asymptotic Sherwood can be approximated by the value corresponding to the constant wall temperature. The dependence of the asymptotic Sherwood number on the geometrical proprieties of the channel is well known [20], being $Sh_{T\infty} = 3.656$ for cells with circular shape and $Sh_{T\infty} = 2.966$ and 2.977 for cells with sinusoidal and square shapes, respectively. In both substrates, the washcoat material leads to round corners and, thereby, the values of the Sherwood numbers of the sinusoidal and square channels approach that of the circular channels.

Fig. 4 shows the Sh_i (i = HC, CO and NO_x) as a function of $ReSc_i(d/L)$ for the ceramic and metallic substrates. The figure reveals that the Sherwood numbers obtained experimentally for both three way catalytic converters operating under real conditions present values lower than the asymptotic *Sh*, regardless of the chemical specie considered. This reveals that the model assumptions that the washcoat is infinitely thin (no internal diffusion limitations) and that the wall reaction is infinitely fast are not satisfied, and thus the conversion is in fact lower than that predicted by considering pure external mass transfer controlled conditions. It does appear that in the case of an automotive catalyst, the conversion, even at high temperatures, is not solely external mass transfer controlled [21,22]. Under these circumstances, the experimental data reveals that the use of asymptotic values for the Sherwood number in 1D models leads to an overestimation of the catalytic converter performance.

Fig. 4 also shows that the Sherwood numbers are chemical species dependent, which, to the best of our knowledge, has not been reported previously. As seen earlier (see Table 1), most studies on mass transfer in catalytic monoliths have been carried out under laboratory conditions, where it is difficult to reproduce the real operating conditions of catalytic converters. It should be noted that Hatton et al. [10] have obtained Sherwood numbers under conditions similar to those used in the present study. These authors have measured HC, CO and NO_x conversion efficiencies, but their experimental correlation for *Sh* has been derived based only on HC and CO measured data – the NO_x data were considered less accurate and thus ignored in the analysis. The measured HC and CO data were grouped together in order to derive their *Sh* correlation Eq. (5).

Eq. (20) reveals that the Sherwood number is dependent of the Reynolds and Schmidt numbers, of the geometrical proprieties of the catalytic monolith and of the NTU. There are two main reasons to obtain different Sherwood numbers for different chemical species: (i) the measured conversion efficiencies are a function of the chemical species, see, *e.g.*, [3,15], which leads to different NTU_i; and (ii) the different diffusion coefficient of the chemical species, which leads to different Schmidt numbers.

Given the typical Reynolds and Schmidt numbers associated to the automotive catalytic converters (see Table 4), it follows, from Eq. (20), that in order to obtain experimentally asymptotic Sherwood numbers it is necessary to have conversion efficiencies higher than 99.99%. In the present study, however, the maximum measured conversion

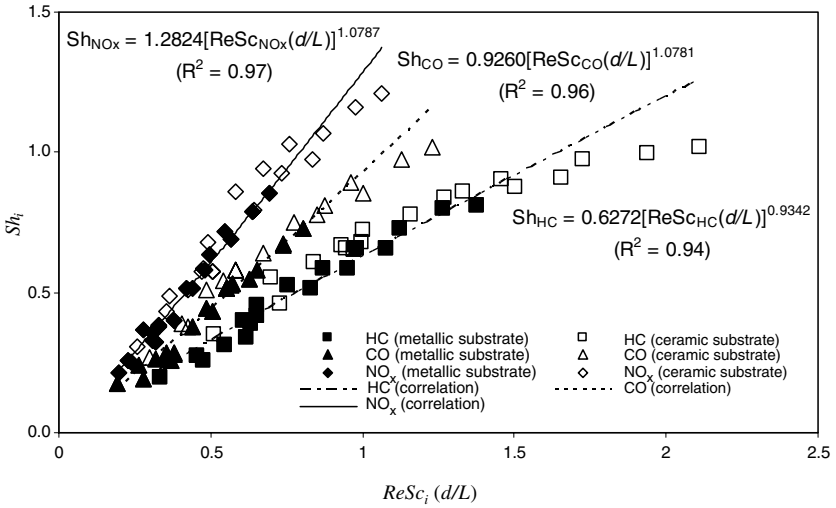

Fig. 4. Sh_i as a function of $ReSc_i(d/L)$.

efficiencies were around 99% and, thus, the measured NTU_i is not high enough to ensure pure external mass transfer control. The difference between the theoretical NTU_i (i.e., NTU_i necessary to reach asymptotic Sh) and the measured NTU_i can be used to quantify the influence of the kinetics and internal diffusion limitations [22]. Our data suggest that the dependence of Sherwood number on the chemical species can be attributed to kinetics and internal diffusion limitations rather than external mass transfer limitations.

Fig. 4 shows that the value of $ReSc_i(d/L)$ for the ceramic substrate is higher than that for the metallic substrate. This is because $ReSc_i(d/L)$ is equal to $16P_i$ and, as pointed out in Section 3, P_i for the ceramic substrate is 53.2% higher than that for the metallic substrate. Fig. 4 also reveals that the ceramic catalytic converter presents higher Sherwood numbers than those of the metallic catalytic converter. Note, however, that for comparable flow conditions, the values of Sh are similar for both substrates. For this reason, the experimental data in the present study have been grouped together for both monoliths, as in Ullah et al. [9]. However, in this study, in contrast with the work of Ullah et al. [9] – that have used only the CO data to obtain their correlation, Eq. (4) – we have also considered the Sherwood number dependence of the chemical species.

Accordingly with the considerations above, the best fit of the present experimental data was obtained with the following correlations:

$$Sh_{HC} = 0.6272\left(ReSc_{HC}\frac{d}{L}\right)^{0.934} \quad \text{for } 0.33 < ReSc_{HC}(d/L) < 2.11 \tag{21}$$

$$Sh_{CO} = 0.9260\left(ReSc_{CO}\frac{d}{L}\right)^{1.078} \quad \text{for } 0.19 < ReSc_{CO}(d/L) < 1.23 \tag{22}$$

$$Sh_{NO_x} = 1.2824\left(ReSc_{NO_x}\frac{d}{L}\right)^{1.079} \quad \text{for } 0.17 < ReSc_{NO_x}(d/L) < 1.07 \tag{23}$$

Fig. 5 shows the present Sh_{HC} along with the ones predicted through Eqs. (1), (2), (3) and (5) as a function of $ReSc_{HC}(d/L)$. The figure shows that the present data agrees well with the results predicted by Eq. (5), derived by [10], see Table 1. It is also seen that Eq. (2), derived by [7], underpredicts slightly the present Sh_{HC} values. This can be attributed to the different nature of the experiments used by Votruba et al. [7] – see Table 1. Finally, Fig. 5 reveals that the results predicted by Eq. (3), derived by [8], are lower as compared with all other results included in the figure. In spite of the temperature range used by Bennett et al. [8] being similar with that of the present study and also of the study of Hatton et al. [10] – see Table 1 – Eq. (3) predicts Sh_{HC} 3–4 times lower than those encountered in these studies. The observed discrepancies can be due to the different hydrocarbons used in the feed streams, as shown in Table 1. In fact, Bennett et al. [8] have used propane that is a saturated hydrocarbon, whereas in present study and in that of Hatton et al. [10] the feed stream was constituted by

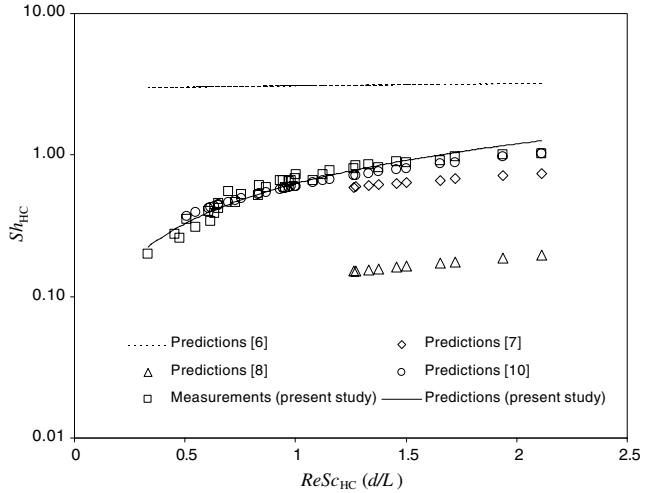

Fig. 5. Predicted Sh_{HC} by various correlations as a function of $ReSc_{HC}(d/L)$.

exhaust gases from a spark ignition engine. The hydrocarbons present in exhaust gases from this device have in their composition 86% of propylene – unsaturated hydrocarbon – and 14% of methane – saturated hydrocarbon [3]. It is well know that saturated hydrocarbons oxidize more slowly as compared with unsaturated hydrocarbons, and therefore the kinetic limitation for the saturated hydrocarbon used by Bennett et al. [8] strongly influence the measured Sherwood number.

Both the present correlation for Sh_{HC} (Eq. (21)) and Eq. (5), derived by Hatton et al. [10], are based on experimental measurements under reacting conditions. As can be seen in Fig. 5, both correlations predict Sh_{HC} below the asymptotic Sh. Hatton et al. [10] showed that Eq. (1), derived by Hawthorn [6], predicts HC conversion efficiencies higher than those measured in their work for high gas temperatures (bulk mass transfer regime). They have concluded that their correlation (Eq. (5)) predicts HC conversion efficiencies more accurately. The present data supports the conclusions of Hatton et al. [10] in that the Sh_{HC} values are lower than the asymptotic Sh.

Fig. 6 shows the present Sh_{CO} along with the ones predicted through Eqs. (1), (2), (4) and (5) as a function of $ReSc_{CO}(d/L)$. As mentioned in Section 1, the correlation derived by Votruba et al. [7] – Eq. (2) – was not obtained for CO oxidation. However, this correlation is the most used in 1D models. Given the experimental ranges of the present work and that of Votruba et al. [7] – see Table 1 – Fig. 6 includes only one point predicted by Eq. (2). As can be seen, the value is close to the values predicted by the others experimental correlations. The figure also reveals that the present data agrees well with the results predicted by Eq. (4), derived by Ullah et al. [9]. Note that the data of Ullah et al. [9] were also derived under reacting conditions for ceramic and metallic monoliths, as in the present work. Both correlations were derived based on the CO oxidation, although the feed streams used

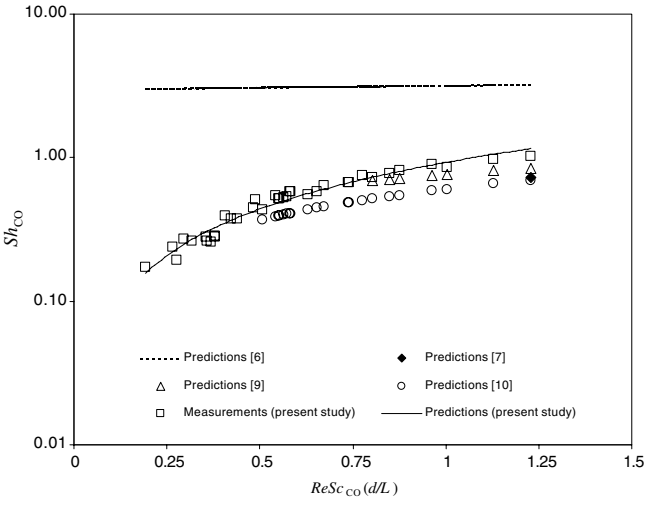

Fig. 6. Predicted Sh_{CO} by various correlations as a function of $ReSc_{CO}(d/L)$.

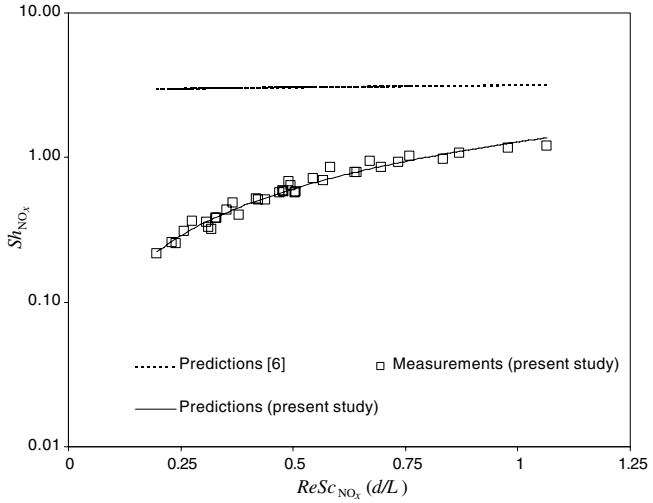

Fig. 7. Predicted Sh_{NO_x} by various correlations as a function of $ReSc_{NO_x}(d/L)$.

were distinct (see Table 1); this can explain the slightly discrepancy observed between the results.

Finally, Fig. 6 reveals that Eq. (5), derived by Hatton et al. [10], slightly underpredicts the present data. This is because these authors have grouped the measured HC and CO data together in order to derive Eq. (5), as mentioned earlier.

Fig. 7 shows the present Sh_{NOx} along with the one predicted through Eq. (1) as a function of $ReSc_{NO_x}(d/L)$. Note that none of the existing correlations available in the literature were derived from NO_x data, and therefore correlations derived from HC and CO data have been often used to predict Sh_{NOx}. For example, Hatton et al. [10] have used their correlation (Eq. (5)) to characterize the external mass transfer process of HC and CO, but for NO_x, given the poor performance of Eq. (5), they have used Eq. (1), derived by Hawthorn [6].

5. Conclusions

This article has concentrated on the analysis of the mass transfer controlled regime in automotive catalytic converters operating under real conditions. The main goal of this study was to evaluate the performance of the existing correlations for the mass transfer rate, expressed as the Sh, against new experimental data and, if necessary, to establish new correlations that can be used in 1D two-phase models. The experiments have included measurements of conversion efficiencies for HC, CO and NO_x from ceramic and metallic three way catalytic converters.

The calculated Sh are always below the asymptotic Sh, which indicates that, in addition to the external mass transfer limitation, both kinetics and internal pore diffusion limitations in the washcoat also contribute to reduce the catalytic converter performance even at the high temperatures encountered in automotive catalytic converters.

The experimental data reveals that Sh's are chemical species dependent, which, to the best of our knowledge, has not

been reported previously. The following correlations for the mass transfer rate were obtained from the experiments: $Sh_{HC} = 0.6272(ReSc_{HC}\frac{d}{L})^{0.934}$, $Sh_{CO} = 0.9260(ReSc_{CO}\frac{d}{L})^{1.078}$ and $Sh_{NO_x} = 1.2824(ReSc_{NO_x}\frac{d}{L})^{1.079}$.

Acknowledgement

The first author (H. Santos) is pleased to acknowledge the Fundação para a Ciência e Tecnologia for the provision of a scholarship (SFRH/BD/32851/2006). The authors would like to thank technician Manuel Pratas who assisted them in conducting the experimental work presented here.

References

[1] H. Santos, M. Costa, Evaluation of the conversion efficiency of ceramic and metallic three way catalytic converters, Energy Convers. Manage., in press.
[2] C. Depcik, D. Assanis, One-dimensional automotive catalyst modeling, Progress Energy Combust. Sci. 31 (2005) 308–369.
[3] S.H. Chan, D.L. Hoang, Heat transfer and chemical reactions in exhaust system of a cold-start engine, Int. J. Heat Mass Transfer 42 (1999) 4165–4183.
[4] V. Balakotaiah, N. Gupta, D. West, A simplified model for analyzing catalytic reactions in short monoliths, Chem. Eng. Sci. 55 (2000) 5367–5383.
[5] G.C. Koltsakis, P.A. Konstantinidis, A.M. Stamatelos, Development and application range of mathematical models for 3-way catalytic converters, Appl. Catal. B: Environ. 12 (1997) 161–191.
[6] R.D. Hawthorn, Afterburner catalysts-effects of heat and mass transfer between gas and catalyst surface, Am. Inst. Chem. Eng. 21 (1974) 849–853.
[7] J. Votruba, O. Mikuš, K. Nguen, V. Hlaváček, J. Skřivánek, Heat and mass transfer in monolithic honeycomb catalysts–II, Chem. Eng. Sci. 30 (1975) 201–206.
[8] C.J. Bennett, S.T. Kolaczkowski, W.J. Thomas, Determination of heterogeneous reaction kinetics and reaction rates under mass transfer controlled conditions for a monolith reactor, Trans. Inst. Chem. Eng., Part B 69 (November) (1991).
[9] U. Ullah, S.P. Waldram, C.J. Bennett, T. Truex, Monolithic reactors: mass transfer measurements under reacting conditions, Chem. Eng. Sci. 47 (1992) 2413–2418.
[10] A. Hatton, N. Birkby, J. Hartick, Theoretical and experimental study of mass transfer effects in automotive catalysts, SAE paper 1999-01-3474 (1999).
[11] R. Giudici, E. Tronconi, Laminar flow and forced convection heat transfer in plate-type monolith strutures by a finite element solution, Int. J. Heat Mass Transfer 29 (1996) 1963–1978.
[12] W.M. Kays, A.L. London, Compact Heat Exchangers, second ed., McGraw-Hill, New York, 1964.
[13] T. Shamim, Effect of heat and mass transfer coefficients on the performance of automotive catalytic converters, Int. J. Engine Res. 4 (2003) 129–141.
[14] N. Baba, K. Ohsawa, S. Sugiura, Numerical approach for improving the conversion characteristics of exhaust catalysts under warming-up condition, SAE paper 962076, 1996.
[15] C.M. Silva, M. Costa, T.L. Farias, H. Santos, Evaluation of SI engine exhaust gas emissions upstream and downstream of the catalytic converter, Energy Convers. Manage. 47 (2006) 2811–2828.
[16] W. Guojiang, T. Song, CFD simulation of the effect of upstream flow distribution on the light-off performance of a catalytic converter, Energy Convers. Manage. 46 (2005) 2010–2031.
[17] G. McCullough, R. Douglas, G. Cunnigham, L. Foley, The development of a two-dimensional transient catalyst model for direct injection two-stroke applications, Proc. Inst. Mech. Eng., Part D 215 (2001) 919–933.
[18] G.C. Koltsakis, A.M. Stamatelos, Catalytic automotive exhaust aftertreatment, Progress Energy Combust. Sci. 23 (1997) 1–39.
[19] R.E. Hayes, S.T. Kolaczkowski, Mass and heat transfer effects in catalytic monolith reactors, Chem. Eng. Sci. 49 (1994) 3587–3599.
[20] F.P. Incropera, D.P. deWitt, Fundamentals of heat and mass transfer, fourth ed., John Wiley & Sons, 1996.
[21] V. Tomašić, Z. Gomzi, S. Zrnčević, Analysis and modeling of a monolith reactor, Chem. Eng. Technol. 29 (2006) 59–65.
[22] C.T. Goralski, J. Goralski, T.B. Chanko, Modeling the effect of substrate cell shape on conversion in monolith catalysts, SAE paper 2001–01–0932 (2001).